

# Molecular dynamics simulation and experimental study on Si<sub>3</sub>N<sub>4</sub>-GCr15 of thin film lubrication

Z Lixiu<sup>1,2</sup>, L Bing<sup>2\*</sup>, W Junhai<sup>1,2</sup>, T Tian<sup>2</sup> and S Qinghua<sup>3</sup>

<sup>1</sup> Testing and Analysis Center, Shenyang Jianzhu University, Shenyang, China

<sup>2</sup> Mechanical College, Shenyang Jianzhu University, Shenyang, China

<sup>3</sup> Party and government office, Shenyang Jianzhu University, Shenyang, China

\* E-mail: 70492819@qq.com

**Abstract.** The molecular dynamics analysis and experimental investigation of thin film lubrication of silicon nitride (Si<sub>3</sub>N<sub>4</sub>) and bearing steel (GCr15) under the n-hexadecane-based lubricant were studied. A molecular dynamics method was used to establish a molecular model with Materials Studio 7.0 software. Forcite module for Geometry Optimization, Dynamics and Confined Shear in three steps. The effects of pressure and velocity on lubrication properties such as van der Waals energy and shear stress of film lubrication were explored. The Rtec friction and wear tester was used to test the Si<sub>3</sub>N<sub>4</sub>-GCr15 friction pair with the change of speed and load.

## 1. Introduction

Si<sub>3</sub>N<sub>4</sub>-GCr15 friction pair is hybrid ceramic ball bearings, which is the most widely used in high-speed electric spindle bearings, that is the rolling body uses hot isostatic pressing Si<sub>3</sub>N<sub>4</sub> ceramic, the inner and outer rings still are the steel ring. Silicon nitride has high strength, hardness and fracture toughness in engineering ceramic systems. Compared with the traditional steel bearing, the hybrid ceramic ball bearing with hot isostatic pressing Si<sub>3</sub>N<sub>4</sub> ceramic has the advantages of high speed performance, high dynamic stiffness, low temperature rise and good thermal stability. Liquid lubricant is now commonly used as a common high-speed bearing lubricant, the lubricant forms micrometer lubricant film on the surface of parts, in-depth study of the characteristics of lubricating films, the molecular dynamics method were introduced. Recent years, molecular dynamics has made great progress in the lubrication, it can essentially reveal the principle of friction lubrication. Shang Shunshi et al [1] used self-design friction tester to test the film lubrication. It was demonstrated that the coefficient of friction was remarkably influenced by rotate speed and contact area of friction under light load, but the influence of the contact area could be neglected under heavy load. Hu Yuanzhong et al [2] used the molecular dynamics simulation to explore the properties of lubricants under thin film constraints which was carried out with spherical molecular fluid. Li yiya et al [3] used molecular dynamics simulation to study the lubrication performance of mineral oil base oil, and found that the role of the base oil molecules to stabilize the lubricating oil film mainly came from van der waals interaction. Bai Minli et al [4] simulated the film lubrication with n-heptane lubricant and investigated the effect of temperature and pressure on the composition, slippage and friction characteristics of the lubricant film. Lv Jizu et al [5] applied molecular dynamics method to study the lubricating effect of nanofluids between two parallel flat walls. Through the analysis of the movement and morphology of the nanoparticles, it



found that the nanoparticles do rotational movement and translational movement under the influence of the wall. The agglomeration of the nanoparticles is very obvious when the pressure is relatively large. The nanoparticles in the fluid effectively played a supporting role in order to separate the friction pair. Sun Yi et al [6] who applied a molecular dynamics simulation established an interaction model of n-hexadecane long-chain molecules used as lubrication to study the friction of the special physical phenomena. The results show that with the change of the shear velocity, the temperatures and shear stresses of the lubricant vary continuously. The phenomena of the delamination and the slippage between the layers of the lubricant appeared at each shear velocity. Zeng Fanlin et al [7] applied molecular dynamics simulations to study the nano-scale thin film lubrication behaviour of two lubricants, pure tridecane and n-tridecane with polyhedron siloxane material  $T_8H_8$  added (the mole fraction of  $T_8H_8$  is 10%), at different shear velocities. Rhykerd et al [8] Hoheisel et al [9] used the molecular dynamics method to calculate the film lubrication with the LJ potential energy function. The results show that the viscosity of the lubricating oil film increases with the increase of molecular dispersion. J.Gao et al [10] used classical molecular dynamics simulation and free energy calculation method to calculate the ultra-thin oil film lubrication, and found that the oil film diffusion and rheological properties are due to the relatively thick layer of 5 or 6 layers in the oil film. I.M.Sivebaek et al [11] studied the kinetic friction calculations of closed hydrocarbon "polymer" solid molecules with molecular lengths between 20 and 1400 carbon atoms to analysed the relationship between frictional shear stress and the shear rate on the different molecular length with two assumptions are made that the polymer slides on the hard substrate and the polymer slides on the polymer. U. Tartaglino et al [12] used the molecular dynamics method to study the lubrication effect of crude surfaces with n-butane and isobutane as lubricants. Tanaka et al [13] studied the dynamic characteristics of the lubricating film between two wall surfaces with the non-equilibrium molecular dynamics simulation (NEMD). JN Ding et al [14] studied the effect of surface roughness on the nanorheological properties of ultra-thin films sandwiched between two solid walls with molecular dynamics simulations. Pinzhi Liu et al [15] used the non-equilibrium molecular dynamics method with branched alkanes as model, studied the relationship between shear viscosity of lubricating oil with temperature and pressure, and received the pressure/viscosity coefficient of base oil molecules. In this paper, n-hexadecane was used as a lubricant to study the influence of pressure and velocity on the lubrication characteristics of  $Si_3N_4$ -GCr15 friction film with the molecular dynamics method, and the correctness of the simulation was verified by experiments.

## 2. Molecular dynamics model and simulation calculation process

### 2.1. Molecular dynamics model and potential energy function

The molecular model of  $Si_3N_4$ , GCr15 and lubricating oil was established by using the Materials Visualizer module. N-dozen alkanes ( $C_nH_{2n+2}$ ) are often used as lubricants for their research on lubricants because their molecular models are relatively close to those commonly used in engineering. The n-hexadecane was established in this paper. Figure 1 is the structure of the model, the two contact surfaces of GCr15 and  $Si_3N_4$  with n-hexadecane are the upper wall surface and the lower wall surface, the positions of the two walls are 29 angstroms and 5 angstroms respectively. In this paper, the shear movement is required to add a vacuum layer of 20 angstroms above the GCr15.

Figure 2 is a molecular dynamics model, the size of the model is  $a = 10.62 \text{ \AA}$ ,  $b = 10.62 \text{ \AA}$ ,  $c = 59.98 \text{ \AA}$ .

The key to accuracy or not of the result of molecular dynamics simulation lies in the selection of the potential function of the interaction between atoms in the system, the potential function is the force field. Many notable discoveries in molecular dynamics simulation of material tribology are based on the L J potential energy function. The L-J potential function is a classical counter-potential function, which can reflect the trajectory of particles. This paper uses the function LJ / 126, the expression of the potential energy function being:

$$V_{LJ}=4\epsilon\left[\left(\frac{\sigma}{r}\right)^{12}-\left(\frac{\sigma}{r}\right)^6\right] \quad (1)$$

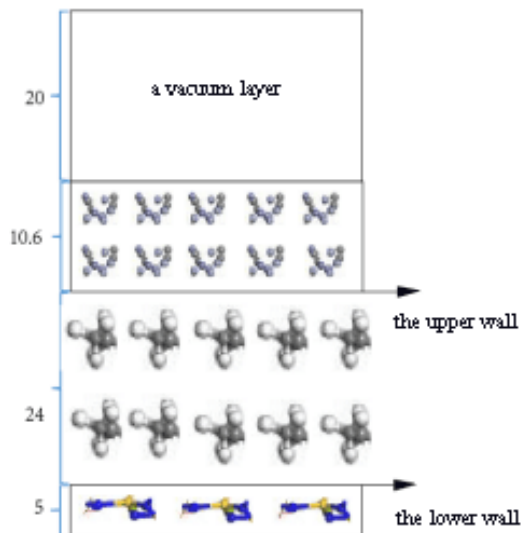


**Figure 1.** Model structure.

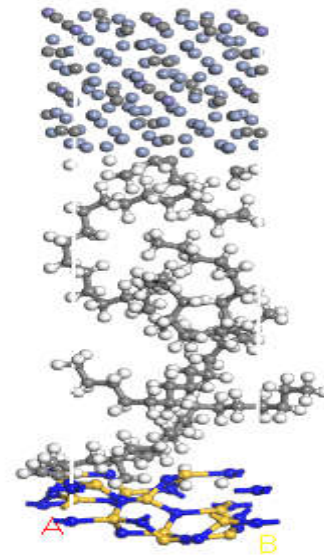


**Figure 2.** Molecular dynamics model.

In the formula:  $V_{LJ}$ -system potential energy, which is van der Waals energy;  $\epsilon$ -the energy parameter ( $r=2^{1/6}\times\sigma$  the minimum energy of the equilibrium position);  $\sigma$ -the length parameter (zero potential energy distance);  $r$ -the distance between atoms.

## 2.2. Simulation and calculation process

The calculation is based on the Forcite module in Materials Studio 7.0, the force field is Universal. Non-bonded truncation of electrostatic interactions and van der Waals interactions using Atom based methods, with a truncation distance of 12.5 Å. The pressure and temperature control functions are the Berendsen and NHL (Nosé-Hoover-Langevin) methods, respectively.

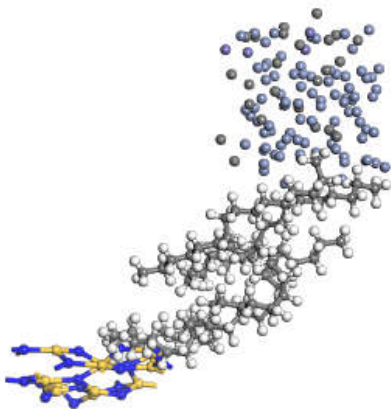
The simulation process is divided into three parts. Firstly, the constructed model is optimized by Geometry Optimization. The algorithm uses the accurate calculation method (Smart) to find the lowest energy conformation of the model, which is used as the simulation and calculation model. Secondly, the optimized model is subjected to kinetic relaxation, which is the equilibrium molecular dynamics simulation process, and the molecular thermal motion is considered. The potential energy model chooses Universal, and the constant temperature and pressure (NPT) is the ensemble. The initial temperature of the simulation is 298K, the pressure is respectively 0.025, 0.051, 0.076, 0.102, 0.127, 0.153, 0.178, 0.201 GPa. The time step is 0.5 fs, the total simulation time is 600 ps. The number of simulation steps is 1.2 million steps and one frame is output every 5000 steps. The process of structural optimization and kinetic relaxation is to balance the model so that the system is in a quasi-stable state for the next calculation. Finally, the non-equilibrium molecular dynamics simulation is performed, that is the shear process. Applying the shear function of Confined shear in Forcite module, the shear rate is applied on the contact surface between n-hexadecane molecules with GCr15 and Si<sub>3</sub>N<sub>4</sub> molecules in the model. The speed of the contact surface is the same and the direction is opposite. Shear velocities are 1.88, 3.77, 5.65, 7.53, 9.42, 11.3, 13.19, 15.07, 16.96, 18.84 Å / ps, respectively. The upper Cr steel and the lower silicon nitride move in opposite directions at a relative speed, which is similar to a frictional process. The potential energy model chooses Universal. The time step selection 0.5 fs, the total simulation time is 6000 ps. The number of simulation steps is 12 million steps and one frame is output every 5000 steps.

Through the combination of different pressure and velocity, various lubrication characteristics of the Si<sub>3</sub>N<sub>4</sub>-GCr15 friction pair film lubrication are obtained. After the simulation is completed, the Analysis function in Forcite is used to analyse the dynamic results and obtain the required data.

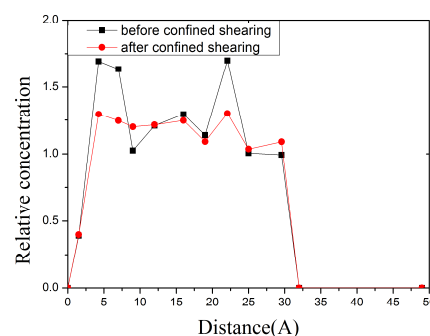
### 2.3. Simulation results and analysis

**2.3.1. The lubrication of n-hexadecane.** Lubrication action of lubricating oil usually comes from the lubrication film formed on the surface of the parts. According to the model of molecular dynamics, it can be considered that the adsorption of n-hexadecane molecules on the surface of GCr15 and Si<sub>3</sub>N<sub>4</sub> molecules. This adsorption is the intermolecular force, which is van der Waals forces. Because the polarity of hydrocarbon molecules is weak, van der Waals forces play a main role, while static electricity can be neglected.

In this paper, the shear movement of n-hexadecane on the surface of GCr15 and Si<sub>3</sub>N<sub>4</sub> is simulated by the confined shear. Figure 3 is a simulation result model under the conditions of 0.102 GPa and 1.88 Å / ps. The distribution of n-hexadecane molecules on the surface of GCr15 and Si<sub>3</sub>N<sub>4</sub> can be observed. Figure 4 shows the distribution of n-hexadecane relative concentration on the surface of chrome steel and silicon nitride with the speed of 9.42 Å / ps and the pressure of 0.102 GPa. The abscissa indicates the distance and the ordinate indicates the relative concentration of n-hexadecane molecules. It can be seen from the figure that the shearing motion has no significant effect on the molecular concentration distribution of n-hexadecane molecules on the surface of GCr15 and Si<sub>3</sub>N<sub>4</sub> either before or after shearing. The two peaks in the graph are approximately at 4.266 and 22.069 angstrom (The change in the wall is due to the pressure exerted by the kinetic relaxation that compresses the entire structure), exactly the surface where n-hexadecane molecules are in contact with the GCr15 and Si<sub>3</sub>N<sub>4</sub> molecules. The two surfaces have the highest concentration of molecules, the concentration between the two is relatively low. Because n-hexadecane produced an adsorption phenomenon on the contact surface, the phenomenon of quasi-solidification appeared, while the middle part still retained the characteristics of the liquid. It is also proved that the alkane molecule can adsorb on the contact surface under the action of van der Waals force and have an important lubricating effect on the part.

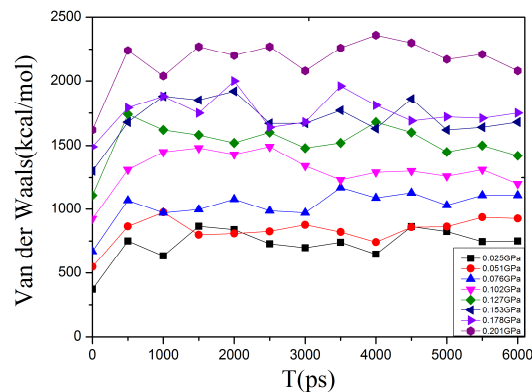


**Figure 3.** Simulation results.



**Figure 4.** Relative concentration distribution of n-hexadecane before and after shearing at GCr15 and Si<sub>3</sub>N<sub>4</sub> surfaces.

**2.3.2. The effect of pressure on thin film lubrication.** The effect of pressure on the lubrication performance of the friction pair was set at 9.42 Å/ps and the pressures were 0.025, 0.051, 0.076, 0.102, 0.127, 0.153, 0.178, 0.201, respectively.

*(1) The effect of pressure on Van der Waals*

**Figure 5.** The curve of van der Waals change with time under different pressures.

In this paper, Van der Waals energy after the final molecular simulation is studied by combining different pressures and speeds. Changing the pressure with the shear rate of  $9.42 \text{ \AA} / \text{ps}$ . Figure 5 shows the changes of van der Waals energy with time under different pressures. The horizontal axis shows the time and the vertical axis shows the van der Waals energy. It can be seen from the figure that Van der Waals can have some fluctuations with the growth of time, but the growth is not much. And with the increase of pressure, Van der Waals can show a rising trend. Because the adsorption of n-hexadecane on the two contact surfaces is gradually enhanced with the increase of pressure, and the lubricating effect of the lubricating oil film on the contact surface is getting bigger and bigger.

*(2) The effect of pressure on the shear stress*

The n-hexadecane has a lubricating effect, but the friction will not be eliminated. Under the shearing motion, shear stress will be generated on the upper wall surface and the lower wall surface in the same direction in the x-direction and in opposite directions.

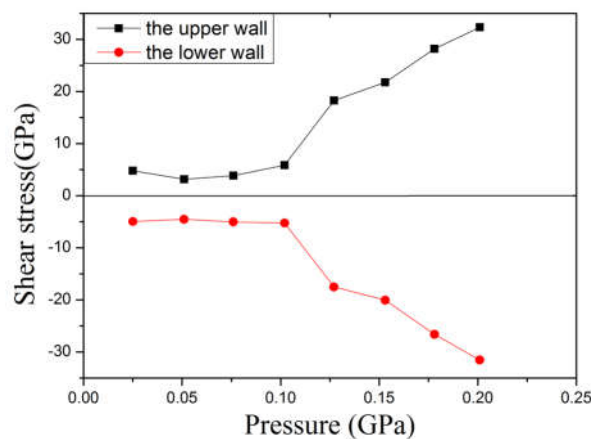


**Figure 6.** The curve of shear stress as time changes.

Figure 6 illustrates the curve of the shear stress with pressure change. It can be seen from the figure that the shear stress on the upper and lower walls is symmetrical. When the pressure is 0.025 GPa to 0.102 GPa, the shear stress changes very little. The tendency of shear stress changes almost linearly and rises rapidly when the pressure is 0.102 GPa to 0.201 GPa. The frictional resistance mainly comes from the internal friction of the lubricating film, that is, the shear force, so the shear flow characteristics of the lubricating film determines the tribological characteristics of the lubrication system. The greater the shear stress, the greater the flow resistance, so the greater the friction.

(3) The effect of pressure on the type of solid film thickness

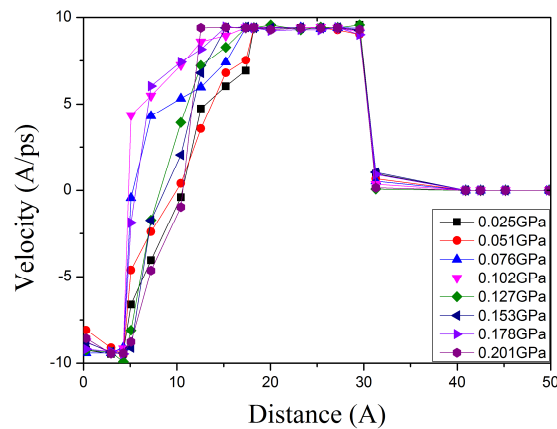


**Figure 7.** Velocity distribution along the thickness of the film at different pressures.

Figure 7 shows the velocity profile along the thickness of the film at different pressures. The abscissa indicates the distance in the film thickness direction and the ordinate indicates the speed. It can be seen from the figure that the curves of speed distribution under different pressures are very similar. At the lower wall 4.266 angstroms and the upper wall 22.069 angstroms, the speed is maintained at  $-9.42 \text{ \AA} / \text{ps}$  and  $9.42 \text{ \AA} / \text{ps}$  respectively. This is because there is a strong adsorption on the two walls, and the velocity is almost the same as the given shear rate. Between 4.266 and 22.069 angstroms, the velocity increases linearly, and the velocity tends to be stable at a certain time, which is consistent with the speed of the upper wall. As the pressure increases, the distance becomes less stable. Because the pressure increases, the liquid film thickness decreases, the thickness of the type of solid film increases.

**2.3.3. The influence of speed on film lubrication.** The effect of speed on the lubrication performance of the friction pair was set at 0.102 GPa, and the speed was 1.88, 3.77, 5.65, 7.53, 9.42, 11.3, 13.19, 15.07, 16.96, and 18.84  $\text{ \AA} / \text{ps}$ , respectively.

(1) The influence of speed on van der Waals energy

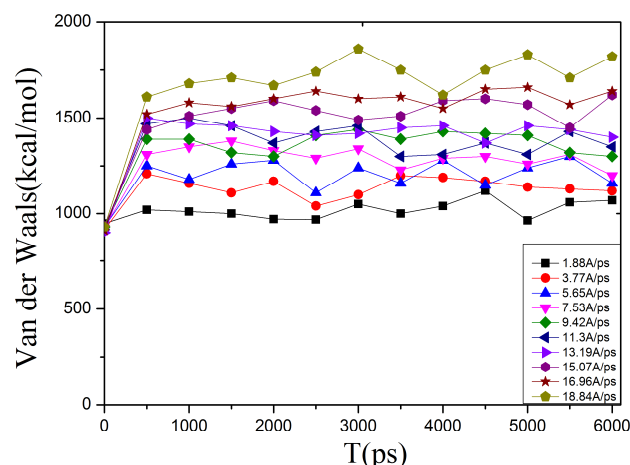


**Figure 8.** Curves of van der Waals at different speeds over time.

Figure 8 is the curve of van der Waals at different speeds over time, that is different speeds. The abscissa indicates the time, and the ordinate indicates the van der Waals energy. The condition of Figure 8 is a fixed pressure of 0.102 GPa, varying at different speeds. It can be seen from the figure

that there will be some fluctuations in the curve with the increase of time, but van der Waals can be seen as unchanged. As the speed increases, van der Waals can show an upward trend. And when speeds respectively at  $1.88\text{\AA}/\text{ps}$  to  $7.53\text{\AA}/\text{ps}$ ,  $9.42\text{\AA}/\text{ps}$  to  $13.19\text{\AA}/\text{ps}$ ,  $15.07\text{\AA}/\text{ps}$  to  $16.96\text{\AA}/\text{ps}$ , van der Waals can be very close. The greater the role of Van der Waals, the greater the adsorption effect.

(2) *The influence of speed on shear stress*

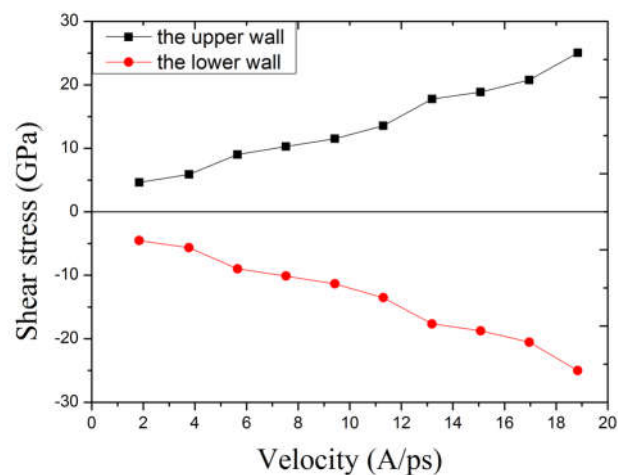


**Figure 9.** The curve of shear stress with the change of velocity.

This paper deals with the shear motion, which produces the same magnitude of shear stress in the opposite direction. Figure 9 shows the shear stress changes with the velocity changes, the abscissa is the velocity, the vertical axis of the shear stress. With the increase of velocity, the shear stress increases. The greater the shear stress, the greater the flow resistance, so the greater the friction.

(3) *The influence of velocity on the type of solid film thickness*

Figure 10 shows the velocity distribution along the thickness of the film at different velocities, the abscissa shows the distance along the film thickness, and the ordinate shows the velocity. It can be seen from the figure that, as the speed increases, the distance from the point of equilibrium tends to be further away from the upper wall surface, and the thickness of the solid film gradually decreases. At  $1.88$ ,  $3.77$ , and  $5.65\text{\AA}/\text{ps}$ ,  $7.53$ ,  $9.42$ , and  $11.3\text{\AA}/\text{ps}$ ,  $13.19$ ,  $15.07$ ,  $16.96$ , and  $18.84\text{\AA}/\text{ps}$ , the points that tend to balance are similar, and the thickness of the solid-like film is the same.

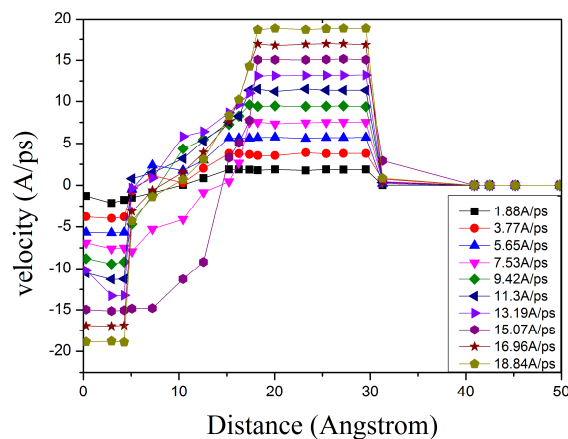


**Figure 10.** Velocity distribution along the thickness of the film at different velocities.

### 3. Experimental investigation

#### 3.1. Test materials, instruments and processes



**Figure 11.** Test materials and oil.

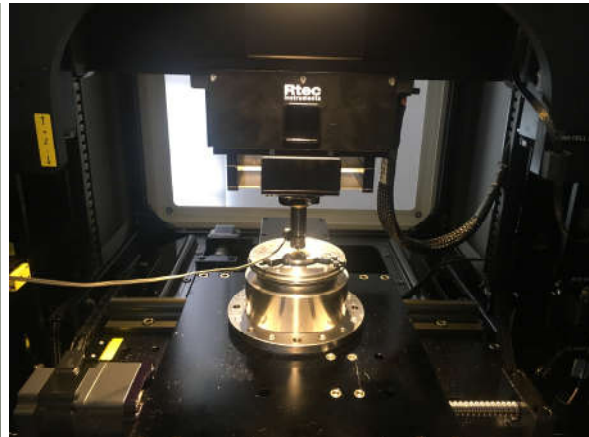


**Figure 12.** Rtec friction and wear testing machine.

On the left in figure 11 is a GCr15 bearing steel disc with a diameter of 50 mm and a thickness of 6.5 mm. In the middle of the hot isostatic pressing  $\text{Si}_3\text{N}_4$  ceramic balls, the diameter is 4.763mm, which is the standard bearing rolling ball size. On the right is the oil used in the test is #32 turbine oil, which has good lubricating properties and proper viscosity. Figure 12 shows the Rtec friction and wear testing machine, this paper applies the rotating module of the testing machine. The top of the graph is the force sensor where the load is applied. The bottom is the rotating module, GCr15 bearing steel disc is fixed on the rotating module. In the middle is the clamping rod, which holds the ceramic ball. In the experiment,  $\text{Si}_3\text{N}_4$  ceramic ball is not moving, the force sensor to impose a certain load on the ceramic ball, making the ceramic ball and bearing steel disc contact. The rotating module takes the bearing steel disc as the radius of the 5mm rotation, and the two forms friction. Test run time is 50 min, the ambient temperature is room temperature, 25 °C or so. The load of test load is from 20N to 160N, which is recorded every 20N. When studying the effect of speed, the load is fixed at 80N. When studying the effect of load, the speed is fixed at 500 r / min. Fixed load and speed are taken in the middle, to avoid the impact of the limit value. Test results can be obtained friction force and friction coefficient by the force sensor.

**Table 1.** Test plan.

Project	Load( N)	Speed( r/min)
first	80	100, 200, 300, 400, 500, 600, 700, 800, 900, 1000
second	20 ,40, 60, 80, 100, 120, 140, 160	500

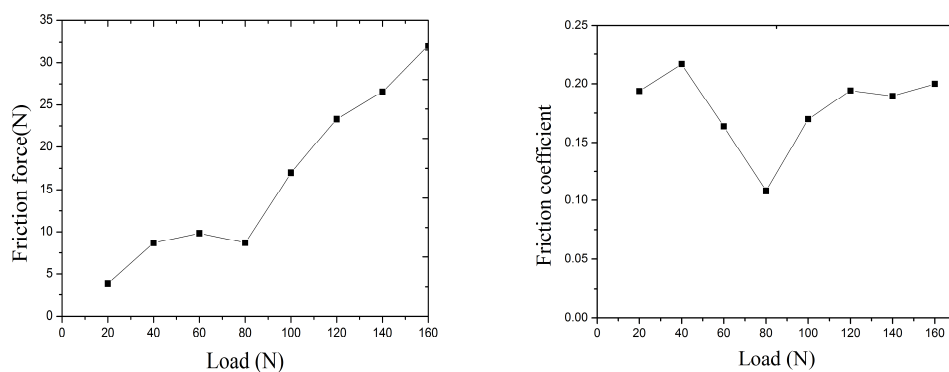
#### 3.2. Test results and analysis

Figure 13 shows the wear scars of different test pieces. The experimental conditions are 500r/min and the loads are 40N, 60N and 100N, respectively. Wear scars of all three test pieces are about 1mm. Although the hardness of  $\text{Si}_3\text{N}_4$  is significantly greater than that of GCr15, the GCr15 disc is worn by the  $\text{Si}_3\text{N}_4$  balls, but the running time is not long, and the contact area does not change greatly from the wear scar, so there is no influence on the test results.



**Figure 13.** Wear scars of different test pieces.

(1) the friction result of the load Change



(a) the curve of friction as the load change.

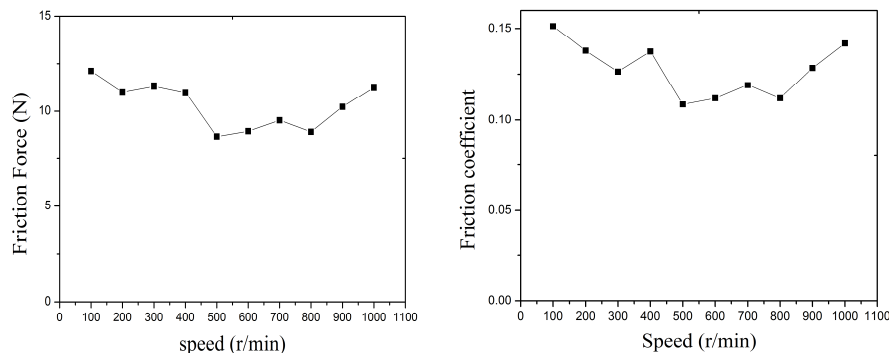
(b) the curve of friction coefficient as the load change.

**Figure 14.** The curve of friction results with load change.

Figure 14 (a) represents the curve of friction as the load changes. The abscissa shows the load, and the ordinate shows the frictional force. (a) shows that the friction increases gradually as the load increases. The curve of friction increases before 80N is gentle, and very steeply after 80N, almost linearly. This is in agreement with the simulation, which initially showed a slow increase in friction and later a rapid growth.

The friction coefficient changes in Figure 14 (b), due to the change of friction. Figure (b) shows the change of the friction coefficient under different loads when the speed is fixed at 500r / min. The abscissa represents the load and the ordinate the friction coefficient. It can be seen that the friction coefficient shows the trend of decreasing firstly and then increasing with the increase of load, and the friction coefficient is the smallest at 80N. Because when the load is small, the lubrication film between the friction pairs of silicon nitride and bearing steel is good, and the friction is reduced, so the friction coefficient is declining; When it drops to a certain value, the increase of load affects the roughness of the contact surface of friction pair, and the friction force increases, so the friction coefficient increases with the increase of load.

## (2) the friction result of the speed Change



(a) the curve of friction as the rotational speed change (b) the curve of friction coefficient with the change of rotational speed

**Figure 15.** The curve of friction result with rotational speed.

Figure 15 (a) shows the curve of the friction with the rotation speed, the abscissa is the rotation speed, and the ordinate is the friction force. It can be seen that the friction decreases first and then increases with the increase of rotational speed, and the friction is the least at 500r / min. And the friction force of 1000r / min is no bigger than 100r / min, this change rule is consistent with the simulation result.

Figure (b) is the curve of friction coefficient with the change of rotational speed and the load is fixed at 80N. Abscissa for the speed, the vertical axis for the friction coefficient. It can be seen that the friction coefficient shows the trend of decreasing first and then increasing with the increase of the rotational speed, and the friction coefficient is the least when the rotational speed is 500r / min. Because of silicon nitride and bearing steel friction pair is dry friction when the speed is very slow. Van der Waals can be smaller, N-hexadecane in the chromium steel and silicon nitride surface does not have a strong adsorption, the film has not been fully formed, the two friction pairs in direct contact, the friction coefficient is bigger. It gradually becomes the boundary friction and fluid friction as the speed increases. Van der Waals can be gradually increased, and the role of intermolecular adsorption increased, forming a stable oil film. Therefore, the friction coefficient of these two kinds of friction is small. The speed continues to increase, the dynamic pressure oil film formation. At this point the friction coefficient is lowest. The speed then continues to increase to reach the mixed friction state, and the friction coefficient increases. However, due to the fact that the final van der Waals can be larger than at the beginning, the friction coefficient is smaller than the dry friction coefficient.

#### 4. Conclusion

Based on the method of molecular dynamics simulation and experiment, this paper studies the lubrication characteristics of the lubrication of  $\text{Si}_3\text{N}_4\text{-GCr15}$  friction film by using pressure and velocity.

(1) The test results show that with the change of pressure, friction force and friction coefficient are the minimum at 80N. With the change of speed, friction and friction coefficient are the minimum at 500r/min. Therefore, the lubrication effect is best when the condition is a load of 80 N and the rotation speed 500 r/min.

(2) The simulation results show that when the pressure is 0.025GPa~0.102GPa, the van der Waals energy and the solid film thickness gradually increase, the friction force remains almost unchanged, and the lubrication effect gradually becomes better; When the pressure is 0.102GPa~0.201GPa, the solid film thickness is very close, although van der Waals can increase, while the friction force increases, the lubrication effect gradually deteriorates. When the speed is 1.88Å/ps~9.42Å/ps, Although the friction force gradually increases, Van der Waals can gradually increase, and the solid

film thickness is larger, so the lubricating effect becomes better; When the speed is  $9.42\text{\AA}/\text{ps}\sim 18.84\text{\AA}/\text{ps}$ , Van der Waals can increase, However, the thickness of the solid film decreases, the friction force increases, and the lubrication effect gradually deteriorates.

## References

- [1] Shunshi S, Jialin G, Feiyu G and Donglin J 2004 Primary influence factors on coefficient of friction in thin film lubrication *Petroleum Processing and Petrochemicals*
- [2] Yuzhong H, Hui W, Yan G, Kun Z and Linqing G 1997 Molecular dynamics simulation of nano-scale liquid lubrication: simulation results of the liquid with spherical molecule *Chinese Journal of Materials Research* **11 (2)** 131
- [3] Yiya L, Jun L, Qinghua D, Zhenyu D, Yi Z and Suo S 2017 Molecular dynamics simulation on the lubricating property of mineral base oil *Acta Petrolei Sinica*
- [4] Minli B, Mei L, Yu W, Jizu L, Zhicheng H and Wang Peng 2017 Molecular dynamics simulation of structure and friction properties of thin film lubrication *Lubrication Eng.* **42 (4)**
- [5] Jizu L, Minli B, et al 2011 The molecular dynamics simulation on impact and friction characters of nanofluids with many nanoparticles system *Nanoscale Research Letters* **6 (1)** 200
- [6] Zeng F and Sun Y 2006 Molecular dynamics simulation of the nano-scale thin film lubrication *Journal of Harbin institute of technology* **38 (9)**
- [7] Zeng F and Sun Y 2006 Molecular dynamics simulation of nano-scale thin film lubrication and its modification *Chinese Journal of Mechanical Engineering* **42 (7)** 138
- [8] Rhykerd C L Jr, Schoen M, Distler D J and Cushman J H 1987 Epitaxy in simple classical fluids in micropores and near-solid surfaces *Nature* **6147** 461
- [9] Hoheisel C, Vogelsang R and Schoen M 1987 Bulk viscosity of the Lennard-Jones fluid for a wide range of states computed by equilibrium molecular dynamics *J. of Chem. Phys.* **87 (12)** 7195
- [10] Gao J, Luedtke W D and Landman U 1997 Layering Transitions and Dynamics of Confined Liquid Films *Phys. Review Letters* **79 (4)** 705
- [11] Sivebeak I M, Samolov V N and Persson B N J Velocity dependence of friction of confined hydrocarbons *Langmuir* **26 (11)** 8721
- [12] Tartaglino U, Sivebeak I M, Persson B N J and Tosatti E 2006 Impact of molecular structure on the lubricants squeeze-out between curved surfaces with long range elasticity *J. of Chem. Phys.* **125 (1)** 469
- [13] Tanaka K, Kato T and Matsumoto Y 2003 Molecular Dynamics Simulation of Vibrational Friction Force Due to Molecular Deformation in Confined Lubricant Film *J. of Trib.* **125(3)** 587
- [14] Ding J.N, Chen J and Yang J C 2006 The effect of surface roughness on nanotribology of confined two-dimensional films *Wear* **260 (1-2)** 205
- [15] Liu P, Yu H, Ren N, Lockwood F E and Wang J Q 2015 Pressure-viscosity coefficient of hydrocarbon base oil Through molecular dynamics simulations *Trib. Letters* **60 (3)** 1